Influence of Corrugation Size and Location on Sensitivity Enhancement for MEMS-Based Pressure Sensor

Seyed Farhan Moosavian, Daryoosh Borzuei, Meisam Farajollahi,*
School of Advanced Technologies, Department of Energy Systems,
Iran University of Technology, Tehran, Iran
**farajollahi@iust.ac.ir*

Mehrad Goharzay
School of Mechanical Engineering, Amir Kabir University of Technology,
Tehran, Iran

ABSTRACT

In this paper, a MEMS capacitive diaphragm-based pressure sensor is investigated. The main focus of this work is to analyze the effect of the geometry and configuration on the sensitivity of a sensor as a crucial parameter in sensor design. Finite element modelling using ABAQUS software is conducted to simulate the behaviour of the diaphragm with different geometries under the same condition. Three popular geometries including square, rectangular and circular shapes with similar areas are investigated and sensitivities of 0.3, 0.24, and 0.22 μm/MPa were obtained for circular, square, and rectangular shapes respectively. Corrugated structure is added to circular diaphragm and deflection and stress analysis are provided for various positions and wave radius of the corrugated region and the best configuration based on sensitivity analysis is proposed. Simulation proved the 17.62% improvement in sensitivity by using a corrugated structure in a circular diaphragm with a small wave radius at the circumference of the circle. An increasing number of corrugated wave regions was also simulated but could not enhance the sensitivity in comparison with a one-wave corrugated structure.

Keywords: *Pressure Sensor; Corrugated Daphragm; MEMS; Sensitivity; Finite Element Analysis*

ISSN 1823-5514, eISSN 2550-164X
© 2022 College of Engineering,
Universiti Teknologi MARA (UiTM), Malaysia.
Received for review: 2020-12-01
Accepted for publication: 2021-06-14
Published: 2022-01-15

Introduction

Nowadays, technological development in the microfabrication industry to create miniaturized Micro-Electromechanically Systems (MEMS) based devices, offers high accuracy, high sensitivity, small size, and low-cost sensors in mass production. Without any doubt, pressure sensors are one of the most common sensors which have attracted a wide range of applications including automotive, gas turbine, aerospace, bioengineering, instrumentation, and petroleum industries [1]. The most typical mechanism of the pressure sensors is based on the deflection of the thin flexible diaphragm as a primary element, which bends due to applied differential pressure. Different methods have been proposed to convert this deflection to measurable quantity including optical technique, piezoelectric and capacitive. Since the development of MEMS technology, piezoresistive diaphragm-based pressure transducers have become the dominant type and maintained their share of the industrial field, due to their stability, high performance, low cost, ease of fabrication, stability, linearity, and repeatability [2]. But in some cases, including high-temperature applications, the capacitive type is preferred because of its high performance and high sensitivity and is also less sensitive to temperature variation [3]. The capacitive pressure sensor consists of two parallel electrodes which one is fixed and one is movable. The movable one that is exposed by external pressure is deformed and this deformation leads to a change in capacitance which is detected and amplified by the designed electrical circuit.

Performance enhancement of this kind of sensors has gained a large number of research and studies to improve their sensitivity, range, and accuracy by changing geometry and shape, material and configuration [4]. Diaphragm shape is one of the effective variables which has been investigated by different researchers to find the best performance regarding maximum tolerable stress, maximum deflection, and best sensitivity [5], [6]. Some of the results show that in the same condition, the circle has less stress and larger deflection which is good for sensitivity compared to squares and rectangles [7]. Suja et al. investigated three different shapes and they showed that the circular shape has better performance but due to the limitations in Very Large-Scale Integration (VLSI) manufacturing, they preferred to work on a square shape. They also used silicon and Silicon on Insulator (SOI) materials for their simulations and compared the results and discovered that these two different materials have different behaviours under various ranges of applied pressure [6].

The maximum deflection at the centre of three different shapes for environmental application is investigated and regarding applied environmental pressure, the different sensitivity was observed [5]. In the range of environmental pressure, using square shape which has larger deflection and smaller stress and also a smaller difference between theoretical formula and Finite Element Model (FEM) simulation has been proposed.

Graphene-based rectangular diaphragm with different dimensions and thicknesses were analysed and observed that stress is directly related to the thickness of the diaphragm, but the effect of thickness is less significant when thickness decreases to 0.25 μm with a length/width ratio of 6. It was shown that this diaphragm is very sensitive to applied pressure and is suitable for applications in miniature, highly sensitive pressure [8].

In another research, silicon carbide has been used as a material for the circular piezoresistive diaphragm and good linearity and sensitivity at the centre of the circle was achieved. In this paper, silicon carbide exhibited 13% better sensitivity in comparison with silicon-made diaphragm [9].

Several materials have been selected and proposed to make diaphragm-based pressure sensors including polycrystalline silicon [10], Graphene [11], SOI substrate with Oxygen ion implantation [12] Germanium [13], Parylene [14], [15], Silicon nanowires [16] and each material and proposed structure has its own advantages and drawbacks.

Configuration as a third important and effective variable also has gained much attention. Thanks to microfabrication progress, different configurations such as corrugated structures are increasingly considered to enhance the performance of the diaphragm-based pressure sensors. Corrugated diaphragms (CDs) have been extensively implemented due to their wider linear range and higher-pressure sensitivity compared to flat diaphragms [17]. Gui et al. observed effective improvement in sensitivity of the circular diaphragm using corrugated structure. They reached 0.44 μm/MPa sensitivity which is two times larger than the same size planar diaphragm [18].

In this paper, three typical shapes of diaphragms are considered after deriving the theoretical formula for stress and deflection and the results are compared to FEM simulation in ABAQUS software. Moreover, the corrugated structure is added to the circular diaphragm, and deflection and stress analysis are investigated as a function of two variables which are position and wave radius of the corrugated region, and the best configuration based on sensitivity analysis is proposed.

Principle of Operation

The sensing mechanism of the diaphragm-based capacitive sensor is based on using the thin diaphragm as a primary element and an electrical circuit as a secondary element to convert the deflection of the diaphragm to a measurable variable. From the structure point of view, it consists of two parallel plates in which the upper one (diaphragm) is subjected to applied pressure and the bottom one is fixed. When the diaphragm with some different shapes such as circle or square is subjected to pressure difference between its two sides, the diaphragm starts to deflect due to the bending moment created by pressure difference and this deflection can change the distance between two parallel

plates. The circumference of the diaphragm is clamped, so the distributed pressure plays a bending moment on the diaphragm and causes tension or compression inside the diaphragm. The capacitance of this capacitor is a function of this distance and is changed due to the deflection of the movable plate. This change is detected and amplified by the designed circuit and converted to an electrical signal [19], [20].

Governing equations:

According to the theory of plates, governing equation to find the deflection of the clamped edges diaphragm is given by:

$$\left(\frac{\partial^2}{\partial x^2}+\frac{\partial^2}{\partial y^2}\right)\left(\frac{\partial^2 w}{\partial x^2}+\frac{\partial^2 w}{\partial y^2}\right)=\frac{P}{D}, \quad D=\frac{Eh^3}{12(1-\nu^2)} \tag{1}$$

where P is applied pressure, w is the deflection of the plate and D is the flexural rigidity of the plate. E, ν, and h are Young's Modulus, Poisson's ratio, and thickness of the plate respectively. Figure 1 depicts the rectangular diaphragm under pressure.

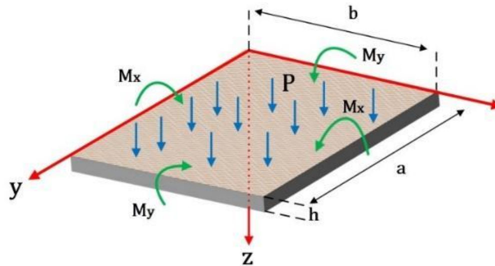

Figure 1: Rectangular diaphragm under distributed pressure.

Solving Equation 1 with clamped edges boundary condition gives the deflection of the plate as a function of position for the diaphragm. Different shapes have different formulas for a deflection which are explained in the following section. When the deflection formula of the plate is known, bending and torsional moments and also normal and shearing stresses can be obtained using mechanics of material formulations:

$$M_x=-D\left(\frac{\partial^2 w}{\partial x^2}+\nu\frac{\partial^2 w}{\partial y^2}\right) \tag{2}$$

$$M_y = -D(\frac{\partial^2 w}{\partial y^2} + \nu \frac{\partial^2 w}{\partial x^2}) \tag{3}$$

$$M_{xy} = D(1-\nu)\frac{\partial^2 w}{\partial x \partial y} \tag{4}$$

$$(\sigma_{xx})_{max} = \frac{\sigma(M_x)_{max}}{h^2} \tag{5}$$

$$(\sigma_{yy})_{max} = \frac{\sigma\left(M_y\right)_{max}}{h^2} \tag{6}$$

$$(\sigma_{xy})_{max} = \frac{\sigma\left(M_{xy}\right)_{max}}{h^2} \tag{7}$$

Maximum stress and deflection of the rectangular, circular, and square diaphragm

Maximum deflection per unit applied pressure is a key factor for the sensitivity of a capacitive pressure sensor. This parameter explains how large deflection is exhibited by the diaphragm under specific external pressure and sometimes is expressed by μm/MPa dimension. Furthermore, we also need to predict when the diaphragm is broken by increasing applied pressure? Or what is the maximum stress which diaphragm can tolerate before the break?

One of the famous criteria is the maximum Von Mises stress which is also known as maximum distortion energy or maximum shear energy theory. This criterion helps one to predict the maximum tolerable stress on a diaphragm and determine the operational range of the pressure sensor [20]. It is possible to use other criteria including the Tresca criterion but due to the relative analysis that is considered in this work and since we want to compare some different cases, it is not very important to use which criterion.

Basically, the Mises criterion represents a critical value of the distortional energy stored in the isotropic material while the Tresca criterion talks about the critical value of the maximum shear stress. Mises criterion or critical distortion energy gives:

$$\frac{1}{2}[(\sigma_1 - \sigma_2)^2 + (\sigma_2 - \sigma_3)^2 + (\sigma_3 - \sigma_1)^2] \le \sigma_Y{}^2, \tag{8}$$

where σ_i and σ_Y are principal stresses and yield stresses respectively. Based on the above equations, maximum stress and deflection formulas are obtained for three different shapes, rectangle, circle, and square to have the ability to compare their behaviour with a focus on sensitivity analysis. To have a reasonable comparison, the total area of each shape is the same. The dimension

of each shape is presented based on π to simplify showing the same sizes. This leads to having the dimensions shown in Figure 2.

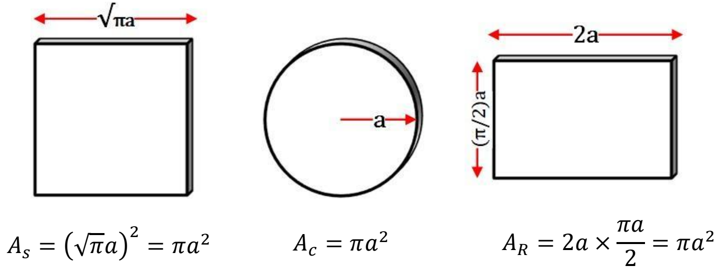

Figure 2: Dimensions of the square, circle, and rectangle shapes diaphragm to have the same area.

Maximum stress at *x* and *y* direction and deflection at the centre for the rectangular diaphragm is given by [21]:

$$(\sigma_{max})_{yy} = \beta \frac{Pb^2}{h^2}, (\sigma_{max})_{xx} = \beta \frac{P\nu b^2}{h^2}, \tag{9}$$

$$w_{max} = \alpha \frac{Pb^4}{Eh^3}. \tag{10}$$

It is worth mentioning that these formulas can be used for square shape as well if the length, a, and width, b, of rectangular is equal. α and β are coefficients determined based on aspect ratio, $\frac{a}{b}$, or dimension of the rectangle. Table 1 shows the values for these two coefficients regarding the rectangle aspect ratio.

Table 1: Coefficient of the rectangular diaphragm to calculate maximum stress and deflection

a/b	1	1.2	1.4	1.6	1.8	2	∞
α	0.0138	0.0188	0.0226	0.0251	0.0267	0.0277	0.0282
β	0.3078	0.3834	0.4356	0.4680	0.4872	0.4974	0.5

For circular shape diaphragm, the maximum stress in *r* (radial) and θ (circumferential) direction and maximum deflection at the centre of the circle can be calculated by [21]:

$$(\sigma_{max})_{rr} = \frac{3Pa^2}{4h^2},\ (\sigma_{max})_{\theta\theta} = \frac{3\nu Pa^2}{4h^2} \tag{11}$$

$$w_{max} = -\frac{3P \times (1-\nu^2)a^4}{16Eh^3}. \tag{12}$$

To model the diaphragm in FEM software, it is required to enter the material properties. In his paper, single crystalline silicon has been selected with E = 180 GPa, ν = 0.28, and ρ = 2330 kg/m^3. Geometric parameters of the circle, rectangle and square diaphragm are shown in Table 2.

Single crystalline silicon which has a diamond cubic crystal structure exhibits completely isotropic behaviour in most properties including thermal and optical properties and also near isotropic in elastic and mechanical properties. It means that assuming this material as an isotropic material is in reasonable approximation [22].

Table 2: Geometrical parameters of the circle, rectangle, and square diaphragm

	Length (µm)	Width (µm)	Thickness (µm)
Square	531.736	531.736	30
Rectangle	600	471.239	30
Circle	Diameter = 300 µm		30

To model the clamped edges diaphragm in FEM software, all nodes at the circumference of the diaphragm have been picked and then all degrees of freedoms (displacements and rotations) for these nodes have been set to zero.

Finite Element Modelling and Simulation

The finite element analysis (FEA) method has been adopted to predict pressure sensor behaviour. A 3D FEA model, for both flat and corrugated membrane, were developed first using commercially available FEA software ABAQUS. The diaphragm analysis has been conducted utilizing the appropriate load and boundary conditions that a pressure sensor experiences. The numerical prediction is then compared with analytical results to validate the FEA modelling scheme. Once the FEA model is validated, additional analyses are conducted for sensitivity analysis as mentioned above. A simple circular membrane is modelled by a 3D shell with 42640 S4 (a 4-node doubly curved thin or thick shell, reduced integration, hourglass control, finite membrane strains) elements and the corrugated membrane is modelled by a 3D shell with

10000 - 48000 S4 elements. Figure 3 shows the meshed diaphragm for the flat and corrugated diaphragm.

Figure 3: An example of a meshed flat and corrugated diaphragm.

Three circular, rectangular, and square diaphragms were subjected to 5 MPa pressure and the results for deflection and Von Misses stress are indicated in Figure 4 and Figure 5.

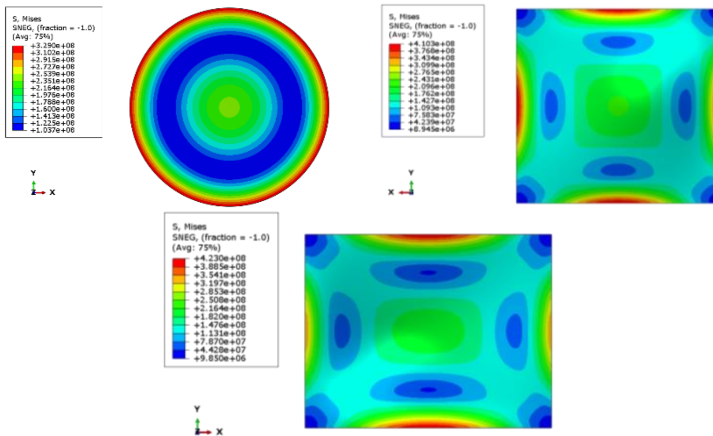

Figure 4: Von Misses stress contour for circular, square, and rectangular diaphragms (units are in meter).

Since the number of elements is not too high and the simulation is not to time-consuming, it was preferred to use 3D modelling and simulation. The boundary conditions considered in this analysis are completely clamped. In other words, all degrees of freedom of the elements around the membrane is clamped and then the load is applied perpendicular to the upper surface of the membrane.

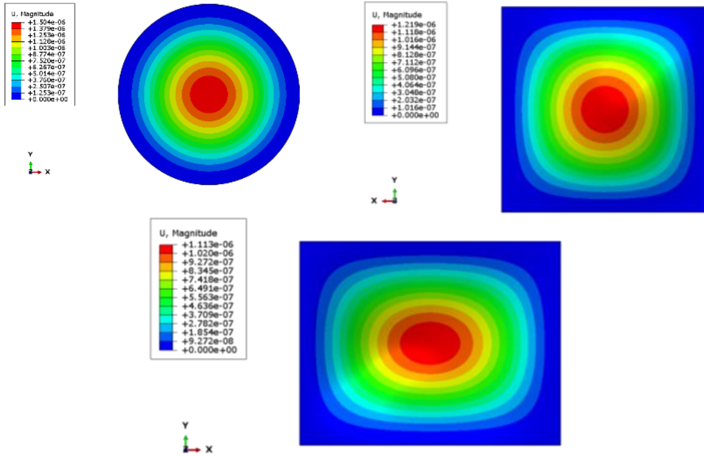

Figure 5: Deflection contour for circular, square, and rectangular diaphragms (units are in meter).

The FEM simulation results are summarized in Table 3. This table gives a comparison of the calculated theoretical results with the FEM results obtained from ABAQUS.

Table 3: Comparison of Von misses stress and deflection results for various diaphragm geometries under 5 MPa applied pressure

	Maximum Von Misses stress (MPa)		Maximum Deflection (μm)	
Geometry	FEM	Theory	FEM	Theory
Circle	329	335.07	1.50	1.44
Square	410.3	432.3	1.22	1.14
Rectangle	423	443.7	1.11	1.02

As can be seen from Table 3, there is a reasonable agreement between calculated theoretical results and FEM simulations. However, the deviation is smaller for circular geometry and is larger for the square one for Von Misses stress. There is a different result for maximum deflection, the smaller deviation belongs to the circle but the larger one is for the rectangle. Interestingly, for all geometries the Von Misses stress from FEM is smaller than the theoretical result but it is inverse for deflection, and we observe the larger value in FEM compared to theory.

Figure 6 shows the stress vs. applied pressure for three different geometries and compares the theoretical results with FEM simulations for pressure variation from 1 to 10 MPa. It is clear from Figure 6 that the maximum

slope for the stress/pressure diagram belongs to square and the minimum one is for circle. It means that in the same applied pressure, the circular diaphragm is subjected to smaller stress which is one advantage of this geometry compared to others and causes a larger pressure range before failure.

Figure 7 indicates the relationship between maximum deflection and applied pressure which is linear as expected from Equations 10 and 12. The slope of Figure 7 is very important because it shows the sensitivity of the sensor which is deflection vs. applied pressure ($\frac{\mu m}{MPa}$). This value is 3, 2.4, and 2.2 for circular, square, and rectangular geometries respectively from the FEM simulations. These values are a bit smaller based on theoretical calculation.

The best matching between theory and FEM has been observed in circular geometry which is another advantage of using circular shape which enables one to predict its behaviour with more accuracy. Circular shape has better performance in comparison with square and rectangle because in the same pressure, smaller stress is induced in a circle and it has larger deflection to pressure ratio which leads to larger sensitivity.

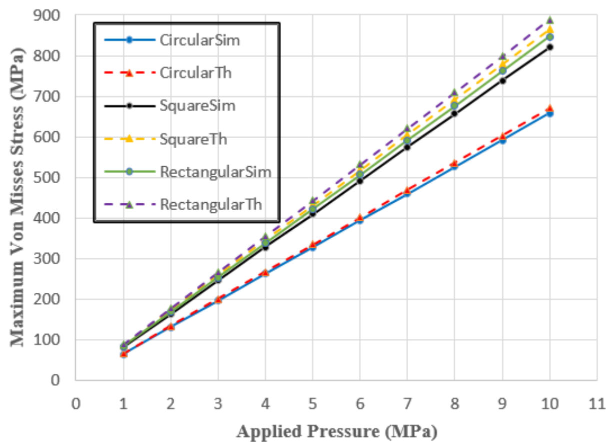

Figure 6: Maximum Von Misses stress vs. applied pressure for three different geometries to compare theoretical results with FEM simulations.

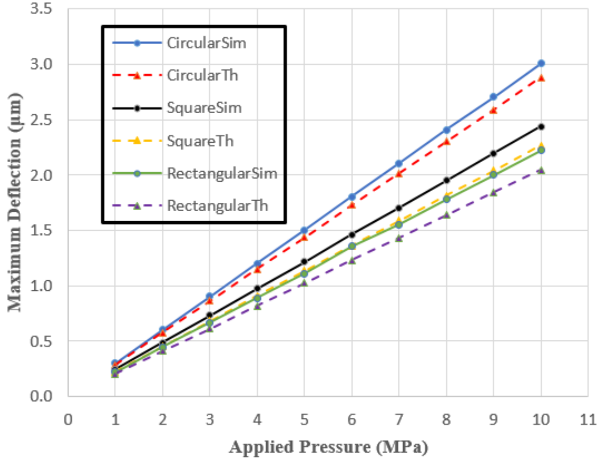

Figure 7: Maximum deflection vs. applied pressure for three different geometries to compare theoretical results with FEM simulations.

Corrugated Circular Diaphragm

Based on the behaviour of the diaphragms under the same conditions, the circular shape is selected because of its unique characteristics including less stress and larger deflection which leads to higher sensitivity for capacitive pressure sensors.

In the next step, the corrugated diaphragm is modelled and deflection, stress, and sensitivity of the CD is simulated using different variables including the position of the corrugated region, *a*, and its radius, *r*. Behaviour of the circular CD is investigated when these variables are changed and the best case for better sensitivity is proposed. Finally, the CD is compared to the flat circular diaphragm and verified that the corrugated diaphragm enables us to enhance the performance of the pressure sensor and significantly improves the sensitivity.

To improve the sensitivity of the circular diaphragm, it is proposed to use a corrugated structure. Specific configuration for the corrugated region at the circular diaphragm is modelled in FEM software and pressure is applied to figure out the behaviour of the corrugated diaphragm. Figure 8 depicts the cross-section of the proposed corrugated configuration for the circular diaphragm.

Figure 8: Proposed corrugated configuration for the circular diaphragm and its cross-section.

In the further simulations, some of the important variables including the position of the corrugated region, *x*, and wave radius, *r*, are changed to find the effect of these parameters on sensitivity and also find the best combination. Figure 9 shows the variables which play important roles in the performance of corrugated diaphragm.

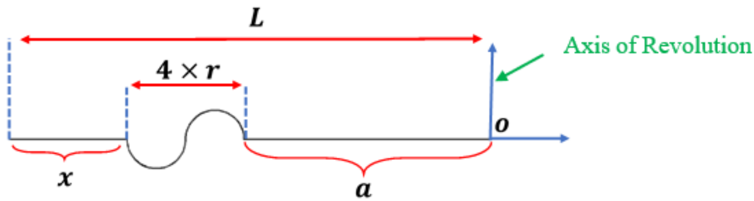

Figure 9: Important variables of the corrugated diaphragm.

To have a correct comparison between the corrugated and flat diaphragm, the projected area which is under external pressure is equal in simulation. When the radius of the diaphragm, L, is 300 µm, then $a = 300 - x - 4r$. To have the same projected area with the flat diaphragm, the variable a, which is the distance of the corrugated region from the centre of the diaphragm, must be selected as calculated in Table 4. For instance, if $x = 200\ \mu m$ and $r = 15\ \mu m$, then a will be 40 µm.

All of the cases presented in Table 4, were modelled and simulated in FEM software to find the best position for placement of the corrugated region with a specific wave radius. As an example, Figure 10 indicates the simulation results for the specific case with $r = 25\ \mu m, x = 0, 100, 200\ \mu m$ under 5 MPa external pressure.

Table 4: Important variable a in the corrugated region designed for the circular diaphragm

$x(\mu m)$ $r\ (\mu m)$	0	50	100	150	200	220	240
15	240	190	140	90	40	20	0
20	220	170	120	70	20	0	-
25	200	150	100	50	0	-	-

It is worth mentioning that a corrugated membrane with circular corrugation is not simple as a flat membrane and the geometry is complex, so there is no analytical formula or rational way to use it in the optimization process. So, one of the best optimization techniques is the trial and error method to find the optimal configuration by FEA software.

Simulation results show that the largest deflection occurs when the position of the corrugated region is closer to the edge of the diaphragm which leads to $x = 0\ or\ a = 200\ \mu m$. But the deflection is not only the parameter to judge the operation and performance of the diaphragm, we need to know the maximum induced stress and also sensitivity.

Since each proposed corrugated configuration has two important variables to change and set (*x, r*), maximum deflection, maximum induced stress, and sensitivity can be drawn as a function of these two variables which creates the 3-dimensional diagrams or a surface shown in Figures 11, 12 and 13.

As can be seen in Figure 10, the maximum deflection happens at the centre of the diaphragm ($x = 0$) when the wave radius is 25 µm. The deflection decreases with decreasing the wave radius and in the case of constant radius, we can find the minimum deflection which is in the middle of the plot at $x \sim 100\ \mu m$.

It is worthwhile to consider that, in the case of induced stress, we are looking for minimum stress which is seen at $r = 25\ \mu m$ and $x = 50\ \mu m$. For the sensitivity plot which is the main aim of this work, maximum sensitivity occurs at the smaller value for both r and x ($r = 15\ \mu m, x = 0$) and the trend of this plot is similar to the deflection plot which was expected.

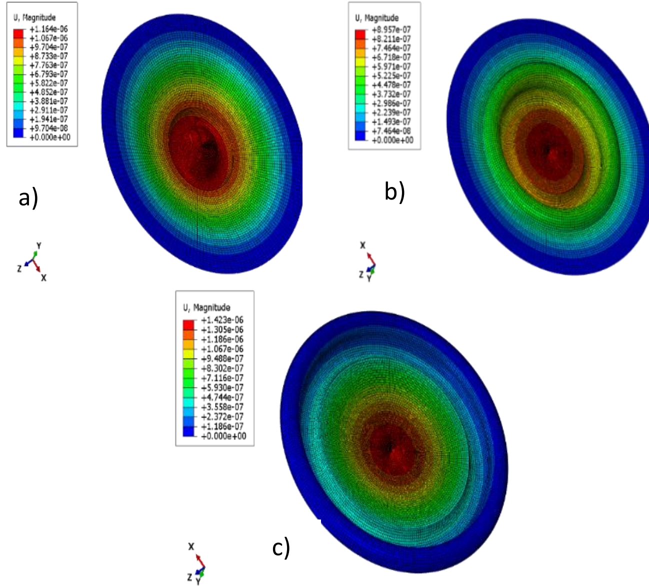

Figure 10: Deflection contour for corrugated circular diaphragm with wave radius, $r = 25\mu m$ and a) $x = 200$, b) $x = 100$ and c) $x = 0$ under 5 MPa external pressure.

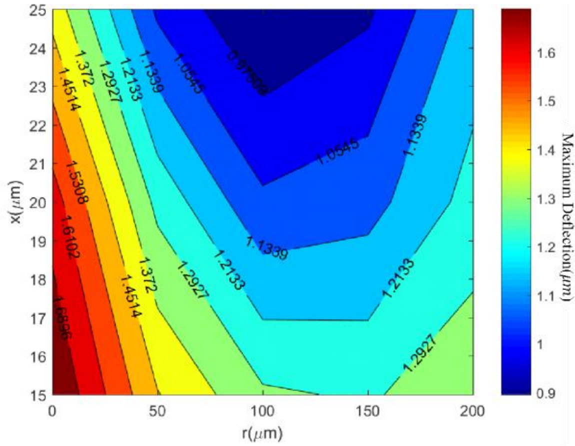

Figure 11: Maximum deflection of the corrugated diaphragm vs. position of the corrugated region, *x*, and wave radius, *r*.

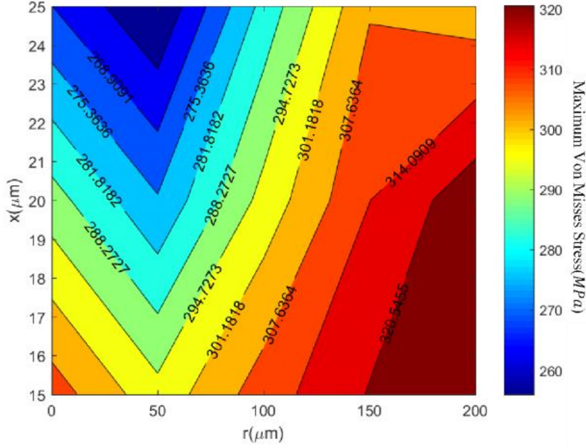

Figure 12: Maximum induced Von Misses stress of the corrugated diaphragm vs. position of the corrugated region, *x*, and wave radius, *r*.

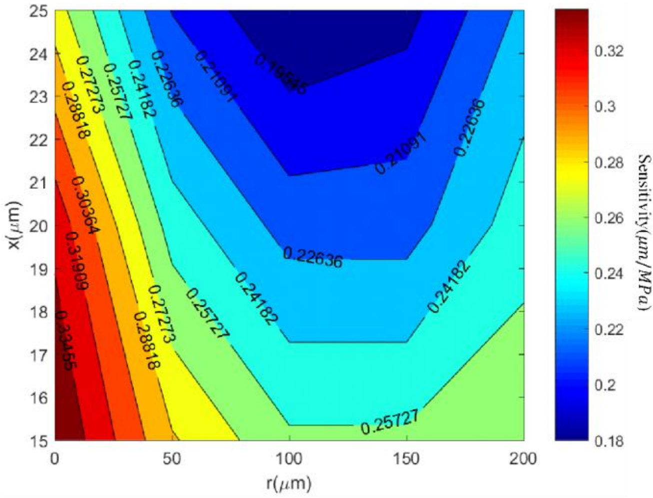

Figure 13: Sensitivity of the corrugated diaphragm vs. position of the corrugated region, *x*, and wave radius, *r*.

As a result, the best case of the corrugated diaphragm based on sensitivity analysis is using a smaller wave radius and pushing the corrugated region to the circumference of the circle. The fabrication of the circular corrugated diaphragm has been discussed in [23], [24]. Reactive ion etching

and low-pressure chemical vapour deposition (LPCVD) are two important steps of the fabrication process.

Results and Discussion

Now, the three typical shapes of the diaphragm and also the corrugated circular diaphragm have been modelled and simulated in FEM software and we are able to compare them together to investigate the improvement of the proposed corrugated structure and verify its advantage against other geometries. Table 5 briefly indicates the comparison between various geometries for maximum deflection, maximum Von Misses induced stress, and sensitivity for diaphragms under 5 MPa applied pressure.

Table 5: Performance comparison of the various geometries for diaphragms under 5 MPa applied pressure

Geometry	Type	Maximum Sensitivity $(\mu m/MPa)$	Maximum Von misses Stress (MPa)	Maximum Deflection (μm)
Circular	Corrugated $(r = 15, x = 0)$	0.3538	310.9	1.769
	Corrugated $(r = 20, x = 0)$	0.33	290.5	1.650
	Corrugated $(r = 25, x = 0)$	0.2846	268.7	1.423
	Flat	0.3	329	1.50
Square	Flat	0.244	410.3	1.22
Rectangle	Flat	0.222	423	1.11

Regarding to Table 5 which is summary of the simulation results, it is observed that the best geometry in case of sensitivity analysis, is corrugated circular diaphragm when the wave radius is smaller and the corrugated region is very close to the circumference of the circle $(r = 15\ \mu m,\ x = 0)$. Pulling corrugated region to the centre of the circle has adverse effect on sensitivity until $x = 100\ \mu m$ and then getting better value again.

Comparing corrugated circle with flat one, verifies the effect of corrugation by decreasing 5.5% induced stress in presence of 17.62% increasing in maximum deflection which leads to 17.62% sensitivity enhancement. It is worth noting that, however using corrugated geometry interestingly improve sensitivity in some cases but, it has adverse effect when

the wave radius goes up and the 5% drop in sensitivity is observable at $r = 25\ \mu m$.

Now, the question is, increasing number of corrugated regions has favourable effect on sensitivity or adverse effect? To answer this question, few number of corrugated regions were created in FEM software. Three various cases were studied which are two-wave corrugated, three-wave corrugated, and four-wave corrugated diaphragms. In the case of two-wave corrugated, there is one wave at the circumference of the circle and another at exactly the centre. For three-wave corrugated diaphragm, one wave is added between centre and edge. For all three cases, the radius of the wave is set to 15 µm. Three modelled configurations are shown in Figure 14.

Figure 14: Three different corrugated diaphragms with different number of waves.

Deflection and induced stress contours for three various corrugated structures are depicted in Figure 15. However, three-wave corrugated structure exhibits better sensitivity compared to two-wave and four-wave configuration but could not improve the sensitivity in comparison with one-wave which has the best performance even versus flat circle diaphragm.

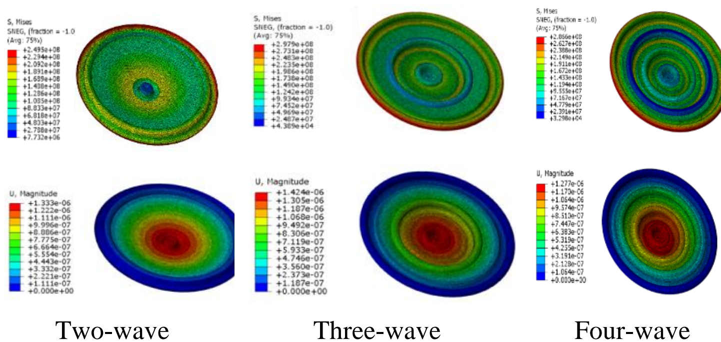

Figure 15: Induced Von Misses stress (Top row) and deflection (bottom row) contours for three different corrugated structures.

As stated earlier, corrugated one-wave configuration with the wave at the circumference, shows better sensitivity compared to all modelled configurations. Simulation results have been summarized in Table 6 for three different corrugated structures.

Table 6: Maximum sensitivity, maximum Von Misses induced stress and maximum deflection for three different corrugated structures

Type of Corrugation	Maximum Sensitivity ($\mu m/MPa$)	Maximum Von misses Stress (MPa)	Maximum Deflection (μm)
Two-wave corrugated	0.266	249.5	1.333
Three-wave corrugated	0.285	297.9	1.424
Four-wave corrugated	0.256	286.6	1.277

Conclusion

In this work, three typical circle, square and rectangle shapes for diaphragm-based pressure sensor were modelled and simulated in FEM software and the results were in reasonable agreement with theoretical formulas proposed in the literature. Then based on sensitivity analysis, comparison between the performances of these three geometries was conducted and circle as a better geometry was selected. To improve the sensitivity of the circular diaphragm, adding corrugated structure to the circle was proposed with specific characteristics. Two important variables were introduced in the corrugated structure (r and x) and the effect of these two variables were investigated through the finite element analysis. Finally, the improvement in sensitivity by using corrugated structure in the circular diaphragm at the circumference with small wave radius was observed and proposed. 17.62% enhancement in sensitivity and 5.5% decrease in maximum stress obtained by implementing proposed geometry. Finally, the effect of increasing number of waves was studied and compared to one-wave corrugated configuration but could not improve sensitivity of the diaphragm.

References:

[1] T. Xu, L. Zhao, Z. Jiang, X. Guo, J. Ding, and W. Xiang, “A high sensitive pressure sensor with the novel bossed diaphragm combined with

peninsula-island structure," *Sensors Actuators A. Phys.*, vol. 244, pp. 66–76, 2016.

[2] A. V. Tran, X. Zhang, and B. Zhu, "Mechanical Structural Design of a Piezoresistive Pressure Sensor for Low-Pressure Measurement: A Computational Analysis by Increases in the," *sensors*, vol. 18, pp. 1–15, 2018.

[3] K. Balavalad and B. G. Sheeparamatti, "A Critical Review of MEMS Capacitive Pressure Sensors," *Sensors & Transducers*, vol. 187, no. 4, pp. 120–128, 2015.

[4] L. Zhao *et al.*, "A bossed diaphragm piezoresistive pressure sensor with a peninsula – island structure for the ultra-low-pressure range with high sensitivity," *Meas. Sci. Technol.*, vol. 27, pp. 1–21, 2016.

[5] A. Nallathambi and T. Shanmuganantham, "Design of Diaphragm Based MEMS Pressure Sensor with Sensitivity Analysis for Environmental Applications," *Sensors & transducers*, vol. 188, no. 5, pp. 48–54, 2015.

[6] K. j Suja, E. S. Raveendran, and R. Komaragiri, "Investigation on better Sensitive Silicon based MEMS Pressure Sensor for High Pressure Measurement," *Intenational J. Comput. Appl.*, vol. 72, no. 8, pp. 40–47, 2013.

[7] N. A. Fathi and Z. A. Moradi, "Design and Optimization of Piezoresistive MEMS Pressure Sensors Using ABAQUS," *Middle-East J. Sci. Res.*, vol. 21, no. 12, pp. 2299–2305, 2014.

[8] S. H. A. Rahman, N. Soin, and F. Ibrahim, "Load deflection analysis of rectangular graphene diaphragm for MEMS intracranial pressure sensor applications," *Microsyst. Technol.*, vol. 24, pp. 1147–1152, 2017.

[9] M. Shaklya, S. Pratyusha, and S. Kumar, "Design , modelling and simulation of MEMS piezo-resistive pressure sensor with clamped edge silicon carbide circular diaphragm," in *International Conference on Internet of Things and Connected Technologies, ICIoTCT*, pp. 706–711, 2018.

[10] V. Musser, J. Suski, and J. Goss, "Piezoresistive pressure sensors based on polycrystalline silicon," *Sensors Actuators A. Phys.*, vol. 28, pp. 113–132, 1991.

[11] S. Zhu *et al.*, "Graphene based piezoresistive pressure sensor," *Appl. Phys. Lett.*, vol. 161904, no. May, pp. 111–114, 2013.

[12] X. Li, Q. Liu, S. Pang, K. Xu, H. Tang, and C. Sun, "High-temperature piezoresistive pressure sensor based on implantation of oxygen into silicon wafer," *Sensors Actuators A. Phys.*, vol. 179, pp. 277–282, 2012.

[13] S. M. Shaby, M. S. G. Premi, and B. Martin, "Enhancing the Performance of MEMS Piezoresistive Pressure Sensor using Germanium Nanowire," *Procedia Mater. Sci.*, vol. 10, no. Cnt 2014, pp. 254–262, 2015.

[14] R. Suzuki, T. V. Nguyen, T. Takahata, and I. Shimoyama, "A Piezoresistive Vibration Sensor with Liquid on Corrugated Membrane," *Proc. IEEE Int. Conf. Micro Electro Mech. Syst.*, vol. 2019-Janua, no.

January, pp. 688–691, 2019.

[15] R. Luharuka, H. M. Noh, and S. K. Kim, "Improved manufacturability and characterization of a corrugated Parylene," *J. Micromechanics Microengineering*, vol. 16, pp. 1468–1474, 2006.

[16] L. Lou, S. Zhang, W. Park, J. M. Tsai, D. Kwong, and C. Lee, "Optimization of NEMS pressure sensors with a multilayered diaphragm using silicon nanowires as piezoresistive sensing elements," *J. Micromechanics Microengineering*, vol. 22, pp. 1–15, 2012.

[17] H. Li, H. Deng, G. Zheng, M. Shan, Z. Zhong, and B. Liu, "Reviews on Corrugated Diaphragms in Miniature Fiber-Optic Pressure Sensors," *Appl. Sci.*, vol. 9, pp. 1-18, 2019.

[18] Y. Gui, Y. Zhang, G. Liu, Y. Hao, and C. Gao, "Design and Simulation of Corrugated Diaphragm Applied to the MEMS Fiber Optic Pressure Sensor," in *IEEE Annual International Conference on Nano/Micro Engineered and Molecular Systems (NEMS)*, pp. 17–20, 2016.

[19] K. B. Balavalad, "Sensitivity Analysis of MEMS Capacitive Pressure Sensor with Different Diaphragm Geometries for High Pressure Applications," *Int. J. Eng. Res. Technol.*, vol. 4, no. 3, pp. 426–431, 2015.

[20] N. Marsi, B. Y. Majlis, and A. A. Hamzah, "The Mechanical and Electrical Effects of MEMS Capacitive Pressure Sensor Based 3C-SiC for Extreme Temperature," *J. Engineering*, vol. 2014, pp. 1-8, 2014.

[21] Z. Niu, K. Liu, and H. Wang, "A new method for the design of pressure sensor in hyperbaric environment," *sensors Rev.*, vol. 37, pp. 110–116, 2017.

[22] D. R. McCarter and R. A. Paquin, "Isotropic behavior of an anisotropic material: single crystal silicon," *Material Technologies and Applications to Optics, Structures, Components, and Sub-Systems,Proc. of SPIE,* vol. 8837, pp. 883707–10, 2013.

[23] F. Ke, J. Miao, and Z. Wang, "A wafer-scale encapsulated RF MEMS switch with a stress-reduced corrugated diaphragm," *Sensors Actuators, A Phys.*, vol. 151, no. 2, pp. 237–243, 2009.

[24] W. Olthuis and P. Bergveld, "The Design, Fabrication, and Testing of Corrugated Silicon Nitride Diaphragms," *J. Microelectromechanical Syst.*, vol. 3, no. 1, pp. 36–42, 1994.